Experimental Investigation of the Effect of *Elaeis guineensis* Mesocarp Fiber on Physical, Mechanical and other Selected Properties of Natural-Fiber Reinforced-Concrete

Odugbose Babashola Dapo, Herni Binti Halim*, Izwan Johari

Abstract—— **In this research study, oil palm mesocarp fiber (OPMF) from the fruit *Elaeis guineensis* was used to produce a natural fiber-incorporated green concrete as a means to reduce the adverse environmental impact of waste disposal and improve the engineering attributes of green concrete. The fiber used was added as a partial replacement for fine aggregate, with percentage variations replaced by volume content. The experiments conducted on the produced OPMF-concrete include physical, durability, morphological, and mechanical properties tests. The OPMF effect in concrete resulted in a slight decrease in density with a range of 2349 kg/m^3 to 2257 kg/m^3, a reduction in workability, and compressive strength range of 45 MPa to 23.17 MPa, a reduction compared to control for all fiber load and fiber size at the 28-day cured specimen for a designed strength of M30. OPMF exerts a reduction in the flexural and splitting tensile strengths, an increase in the porosity of the concrete, and, likewise, a high chloride penetrability with charge values greater than 4000 coulombs. Due to the randomly dispersed fiber particles, hydration of the binder was restricted, and the fiber made more pore spaces available, creating a less dense structure. Moreover, the presence of OPMF in the microstructures of fiber-concrete decreases the bond between the binder and the aggregates.**

Index Terms— **Agricultural Waste Management, Compressive Strength, Fiber-Sand Replacement, Sustainable Green Concrete.**

I. INTRODUCTION

Nowadays, researchers worldwide, particularly in developed countries, are concerned with sustainable development and environmental safety. The use of construction materials is critical for the long-term development of buildings. These materials can significantly impact energy consumption, carbon dioxide emissions, landfills, and natural resource conservation [1-4]. The critical issues in the construction materials industries are primarily related to the depletion of natural aggregates, the extensive use of ordinary Portland cement (OPC) and associated excess CO_2, waste production and destruction, and landfill space scarcity [5-7]. Concrete has been the most commonly used construction material for many years, with global production exceeding one tonne of concrete per person on the planet [8]. Buildings have been identified as a significant contributor to the environmental impacts of human activities. Most buildings are constructed entirely of concrete and other cement-based materials, which impacts the environment. One approach to reducing these negative impacts and ensuring the construction industry's long-term development is to seek new materials and construction systems with renewable components, low energy costs of production and application, and low pollutant emissions during production [9-11]. Many researchers have replaced these building materials with natural, renewable, and recycled options to limit greenhouse gas emissions, conserve natural resources, and improve building environmental performance [12-18].

To combat environmental issues and save energy, recycled and waste materials are increasingly used in concrete. The improvements in concrete properties, as well as the environmental benefits from the use of waste materials, encourage further research into the production of green concrete. Several alternative and waste materials, such as construction and demolition waste [19], fly ash [20], and marble waste [21], are examples of waste materials. Silica fume (SF), natural pozzolan, ground granulated blast furnace slag (GGBFS) [22], paper industry sludge waste [23-24], silico-manganese fume [25], acai' fibers [26-27] were added to improve the properties of mortar or concrete, glass powder waste [28], nano-silica, cement kiln dust, electric arc furnace dust [29], granite residues [30], ornamental stone-processing waste [31], wind turbine blade waste [32], and kaolinitic clay [33] have been used in mortar or concrete to improve their properties, save energy, and reduce greenhouse gas emissions. Concrete is exceptionally brittle and thus performs poorly under tension; several materials have been incorporated to increase ductility and produce a more durable concrete material to mitigate brittleness. Steel is the most common of these materials

Manuscript received June 15, 2023; revised October 23, 2023.

This work was supported by Universiti Sains Malaysia (USM) through the Research University Individual-RUI Grant (1001/PAWAM/8014161).

Odugbose, B.D is a PhD candidate of the School of Civil Engineering, Kampus Kejuruteraan, Universiti Sains Malaysia, 14300, Nibong Tebal, Pulau Pinang, Malaysia. (e-mail: odugbose.babashola@student.usm.my; odugbosebabashola@yahoo.com)

Herni Halim is a Senior lecturer in the School of Civil Engineering, Kampus Kejuruteraan, Universiti Sains Malaysia, 14300, Nibong Tebal, Pulau Pinang, Malaysia. (corresponding author phone: +6-04-5996247 Email: ceherni@usm.my).

Izwan Johari is a Senior Lecturer in the School of Civil Engineering, Kampus Kejuruteraan, Universiti Sains Malaysia, 14300, Nibong Tebal, Pulau Pinang, Malaysia. (e-mail: ceizwan@usm.my).

because it is ductile and is typically used as primary reinforcement. Steel fibers are also used as secondary reinforcement in reinforced concrete at times. The goal of incorporating reinforcing materials into concrete, in whatever form they take, is to improve ductility and prevent brittle failure. Aside from steel, other materials used to improve concrete ductility include fibers, typically randomly distributed in a concrete matrix. However, the ongoing cost, energy demand, and environmental impact of infrastructure have necessitated the search for alternatives to traditional structural reinforcements such as steel. Although steel has numerous advantages when used in cement composites, it is both expensive and unsustainable in terms of the environment.

In order to mitigate the environmental impact of the continuous use of non-renewable fibers in composite concrete, efforts are being directed towards using natural fibers as they gain ground in new approaches to building designs and development as the use of natural and local building materials gains strength [34]. Due to their low density, low embodied energy, economy, and environmental sustainability, fibrous and porous materials of plant origin are increasingly finding applications in the construction industry [35-36]. These fibers are widely available, significantly less expensive to process, and environmentally friendly. Engineers, researchers, and scientists have focused on using sustainable materials in the construction industry [37-41]. Several benefits of using natural fibers in cement composites have been reported in the literature. These benefits include low cost, zero carbon footprint, lightweight, toughness, biodegradability, non-toxicity to the ecosystem, and high recyclability [42-44]. According to the Food and Agriculture Organization (FAO) publication on global agriculture towards 2050 [45], the world's population is expected to grow by more than 2.3 billion people (i.e., more than a third of the current population) by 2050, with the developing world accounting for the majority of this growth. The implication is that agricultural activities will also increase. Aside from the anticipated increase in agricultural waste [46-50], one of the implications is the expected strain on already-scarce infrastructure.

Agricultural waste fibers have been used as reinforcements in concrete, with jute fiber increasing the compressive strength of the produced concrete [51]. Miscanthus fiber reduces the compressive strength of concrete produced with it [52]. Bamboo fibers in concrete reduce the workability and quality of the concrete while increasing the suppression of crack growth and propagation [53]. Using flax fiber in concrete increases the strength and toughness of the concrete [53]. According to [54], hemp fiber in concrete improves fire resistance. The incorporation of coconut fiber in a high-strength superplasticized concrete by [55] increased compressive strength, modulus of elasticity, and splitting-tensile strength at an optimum inclusion of 2%. A 5% weight addition of banana fiber raises the flexural toughness index but lowers the modulus of rupture [56].

Another source of natural fiber is oil palm mesocarp fiber, which is derived from the oil palm tree, a major economic crop in many countries. Oil palm is a significant agricultural crop in Malaysia, accounting for the fourth most prominent contribution to the country's GDP [57-58]. Every year, Malaysia produces millions of tonnes of oil palm fibers (OPFs) [59]. Oil palm empty fruit bunch (OPEFB), oil palm mesocarp fiber (OPMF), palm kernel shell, and palm oil mill effluent are examples of mill OPFs. OPFs are regularly cut and collected in plantation areas while harvesting fresh fruit bunches and palm tree pruning [60]. OPMF is used as a fuel in mill steam boilers. However, due to its large quantity, it could be used more efficiently. OPEFB is typically inexhaustible, with only 10% available for other uses [61]. Meanwhile, OPF is felled in between the interrow of oil palm plants because, once decomposed, it is reused as a high-nutrient fertilizer [57]. Researchers are very interested in biomass generated by oil palm industries because it is abundant and can be converted into value-added materials. From the standpoint of environmental sustainability, using Oil Palm Mesocarp Fiber in concrete is encouraged because it conserves mineral resources, reduces the high carbon footprint due to incineration in boilers, and reduces the need for new landfills required for disposals. There is also little to no data on the effects of using oil palm mesocarp fiber on concrete properties, so this experiment aims to determine the outcome of the influence of using oil palm mesocarp fiber on concrete.

II. MATERIALS AND METHODOLOGY

A. Materials

Panda Portland Cement MS EN 197-1: 2014 CEM I 52.5 N, supplied by Hume Cements Sdn Bhd Selangor Daru Ehsan, Malaysia, was the binding material in the concrete mixes. The oil palm mesocarp fiber used as partial replacement of the sand in concrete constituents by volume. The fiber was gathered from oil palm refineries at Nibong Tebal and Jawi, both within Seberang Perai Selatan, Pulau Pinang, Malaysia. River sand was sourced from a local natural river within Nibong Tebal. Sieve analysis of the river sand was carried out per standard ASTM C136/C136M-14 [62]. The specific gravity value of 2.65 and the fineness modulus of 3.36 were obtained for the river sand, while the specific gravity of 0.89 was obtained for the mesocarp fiber, respectively. The coarse aggregate of specific gravity of 2.67 used was from crushed gravel with max size 20 mm, sourced locally and free from deleterious materials. Sieve analysis was conducted to grade the coarse aggregate according to ASTM C136 [62].

B. Mix Design

The natural fiber composite concrete (OPMF-concrete) was made following the standard of ACI 318 [63], where the water-cement ratio (w/c) is 0.45. The desired compressive strength of the specimens is set at 30MPa with workability of 60 mm to 80 mm. Many batches of the concrete mix were produced with the different substituting fiber particle sizes of three distinctive particle sizes, nomenclature A, B, and particle C, respectively. Table 1 presents the detailed mixes for the different mixes, with each mix repeated for the three distinct fiber particle sizes A, B, and C, respectively, with concrete constituent proportions derived from the design mix using the stated standard as 440.5 kg/m³, 714 kg/m³, 1024 kg/m³ and 196 kg/m³ for cement, fine aggregate, coarse aggregate, and water content respectively in $1m^3$ concrete mix. The table shows a mix for the control specimen in which no fiber was added, as well as a constant value for cement, water, and coarse aggregate, while the

acceptable aggregate and fiber particle inclusion varied by the percentage replacement of the fine aggregate in each mix respectively in volume content replacement.

TABLE I
COMPOSITION OF CONCRETE MIX AT CONSTANT W/C (0.45)

Sample	Cement kg/m³	River Sand (kg/m³)	Coarse Aggregate kg/m³	Weight (%)	Fiber Weight kg/m³	Water kg/m³
OPC0	440.5	714	1024		0	196
OPMF2	440.5	699.7	1024	2	4.796	196
OPMF4	440.5	685.4	1024	4	9.592	196
OPMF6	440.5	671.2	1024	6	14.388	196
OPMF8	440.5	656.9	1024	8	19.184	196
OPMF10	440.5	642.6	1024	10	23.980	196

C. Specimens Preparation

Regular concrete with no additional fiber was produced and made as the control specimen in order to determine the impact of the addition of fiber on the properties of the composite-concrete produced with OPC0 represents the control samples mixes for compressive strength, flexural strength as well as splitting tensile respectively while OPMF2, OPMF4, OPMF6, OPMF8, and OPMF10 represents the mixes containing 2%, 4%, 6%, 8%, and 10% of oil palm mesocarp fiber as partial replacement of river sand by volume respectively. These percentage replacements were carried out for compressive strength specimens and flexural strength and splitting tensile samples, respectively, following the mold dimensions for the various testing specimens. It is worthy of note that these mixes were carried out for three distinct particle sizes A, B, and C, representing 0 – 1.18 mm, 1.19 mm – 2.36 mm, 2.37 - 5 mm, respectively (see Fig 2a), with all sizes within the particle size range of fine aggregate in the standard concrete.

Following the various planned proportions of the concrete constituents, the river sand and cement were mixed first in the concrete mixer for 1 min, followed by adding the fiber. Then, it was mixed for an additional 1 min. Coarse aggregate proportion is then added to the mixed contents (cement, sand, and fiber) in the mixer and allowed for a further 1min of thorough mixing. Water was then added gradually in bits while the mixing was ongoing until a homogenous mixture was obtained, arriving at a total mixing time of about 5-7mins (See figure 2b and 2c). The prepared OPMF-concrete was cast inside molds of varying dimensions as required for the different testing (fig 2f) and was agitated on a electrically operated vibration table to attain consolidation while been placed in three layers with each layer placement agitated. Samples were left in the mold for 24 hours, covered with a moist jute sack (damp hiessen). All specimens were removed from the mold after 24hrs (fig 2d) and cured in water curing tanks following ASTM C 192/ C192M [64] and EN 12390-2 [65] (see fig. 2g).

D. Testing

Testing for the workability of the fresh concrete was carried out using the conventional slump cone test. After proper mixing, the fresh concrete was subjected to a slump test per ASTM C143/C143M [66]. The effect of fiber addition to concrete on workability was also conducted following the above slump testing standard (see Figures 1a and 1b). The density of control concrete and fiber composite concrete were determined under ASTM C642-13 [67], taking the average value of the 3 specimens at each percentage fiber-fine aggregate replacement; likewise, the water absorption properties followed the same standard.

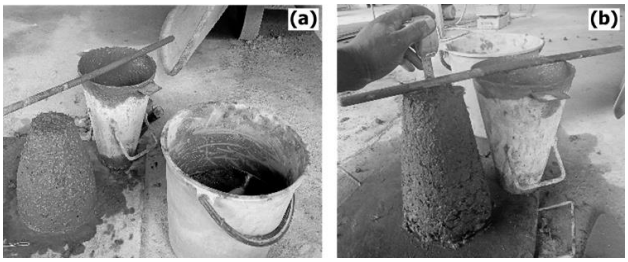

Fig 1: Slump test for (a) C6 and (b) C10

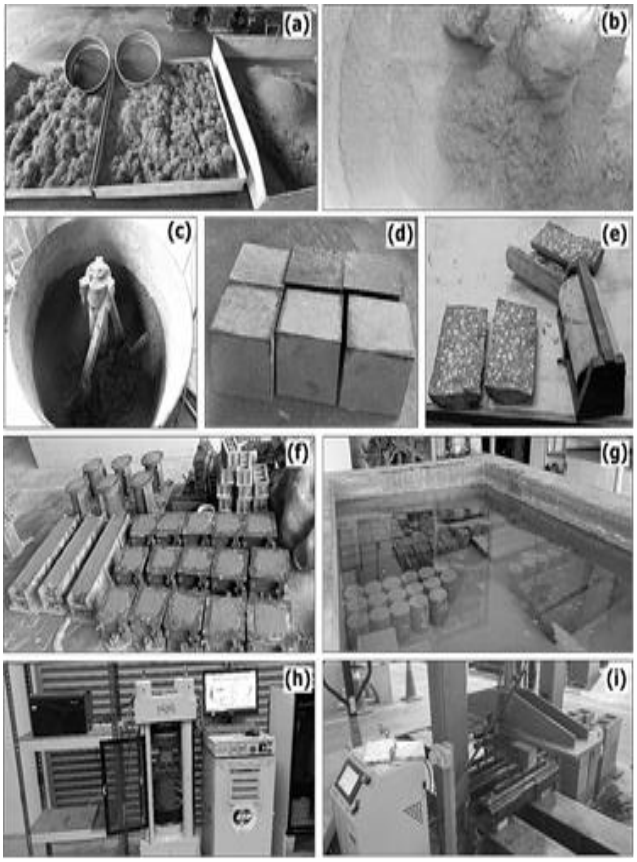

Fig 2: Procedural diagram showing (a) three distinct fiber particle sizes A, B and C, (b) dry mixing of materials, (c) well-mixed wet OPMF-concrete, (d) de-molded compressive strength specimens, (e) splitting tensile strength testing, (f) specimens in molds, (g) curing of specimen in water tank, (h) compressive strength testing, and (i) flexural strength testing.

The mechanical properties of the casted OPMF-concrete were determined in the laboratory after curing in a water tank at ages 7, 14, 28, and 56 days for compressive strength specimens with 100 mm * 100 mm * 100 mm dimensioned specimens. The test was conducted on Universal Test Scientific, Unit Test Compression Machine (Unit Test Scientific) Mac Type: CUT 300/50 EN, Serial No: C235/1W30/5 CEN-A170813, Max Cap: 3000 kN, Weight: 900 kg in accordance to BS EN 12390-3 [68] (see fig 2h). Flexural test specimen (beam: 100 mm * 100 mm * 500 mm) was tested at age 28 days curing on flexural strength machine LIYA LABORATORY TESTING EQUIPMENT, 7" Touch Screen, TFT Control Panel, supplied with Automatic Hydraulic Power Unit with Serial No.: 21/00389, Device Code: LT-C0226, Voltage: 220-240, Weight: 85kg

Ampere: 3A, Hz: 50 – 60, Capacity: 100 kN machine operated on a four-point beam loading test with the pace of 0.26KN/s loading in accordance to ASTM C 78-02 [69] (see fig 2i). Splitting tensile test specimens (Ø100 mm * 200 mm height specimen) undergo testing using the Pro-Equip Split Tensile Component with test gauge, Accuracy ± 0.5% FSD, Scale Division = 5kN, Serial No.: 140529976, 500 kN capacity mounted on Compression Machine manufacture by WYKEHAM FARRANCE WF 55200, Serial No: 69117-1, Capacity: Max. 2000 kN machine operated on 3kN/s loading, carried out on cylindrical specimens in accordance to ASTM C 496/C 496M – 04 [70] (see fig 2e).

SEM test was conducted on the sample using specimen dimension 1 cm * 1 cm fixed on the holder with a sticky carbon tape (see Fig. 3) with the test conducted in an FEI QUANTA FEG 650, serial number D9817 Scanning Electron Microscope machine recorded at 5kV with 250x and 1000x magnification, while the EDX was obtained using the same machine at the same magnification.

The effect of the incorporation of OPMF into concrete on chloride permeability was tested using 3 specimens of each particle size and percentage of fiber replacement. Cut out from a cylinder specimen into Ø100 mm * 50 mm, vacuumed, pressured dry for 3 hours, and then subsequently submerged in water for additional vacuumed pressure for another 6 hours to attain saturation. After 6 hours of submerged vacuum, the specimen was left in the submerged water for 24 hours before carrying out the test per ASTM C1202-05 [71], with each test duration of 6 hours. Fig 4 shows the testing setup.

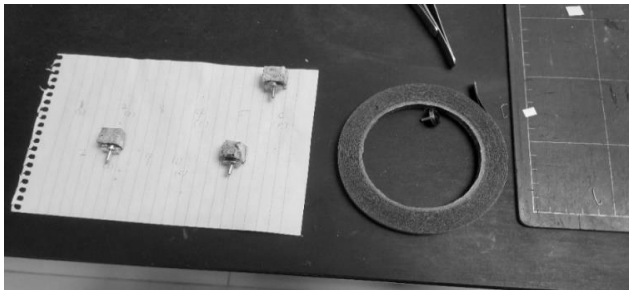

Fig 3: SEM prepared specimens

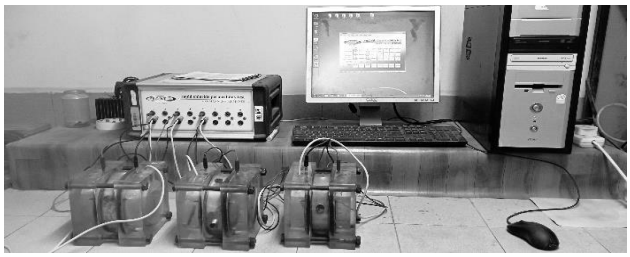

Fig 4. RCPT set-up

III. RESULTS AND DISCUSSION

A. Concrete Workability

The OPMF's effects on the fiber-composite concrete's workability are presented in Fig. 5. This result looks at the corresponding effects of fiber addition in replacing fine aggregate across all the percentage replacements and the fiber particle sizes. From the graph, it can be deduced that the workability of fresh OPMF-concrete is reduced compared to that of non-included fiber. The slump value obtained for the control specimen was 132.08 mm, while those obtained for the OPMF-concrete reduces from these values. As shown in fig 5, a consistent pattern of slump reduction across all percentage replacements and particle sizes. Consistent percentage reduction of the slump compared to plain concrete ranges from 49% at 2 % fiber inclusion to 97.73% at 10% fiber inclusion for particle size A. As for particle size B, the reduction percentage of a slump is between 22% at 2% and 98% at 10% fine aggregate replacement. Particle size C shows a similar pattern of slump value reduction, with a range of 43.2% reduction from 0% to 2% fine aggregate replacement and a gradual reduction from this percent to 96.2% at 10% fine aggregate replacement. The pattern from the graph shows that as the percentage of fine aggregate replacement increases, there exists a corresponding reduction in the workability of the fiber-concrete produced.

This phenomenon can be associated with the hydrophilic nature of the fiber added, as it tends to absorb water into its microfibrils, thereby reducing available water, as evident from the sharp reduction in slump. As the percentage of fiber inclusion increases, there is a high need for water as the randomly distributed fibers consume the free water within the samples, thereby causing a reduction in fluidity. This reduction trend in a slump is similar to that obtained by other research with natural fiber inclusion in concrete samples (72-75).

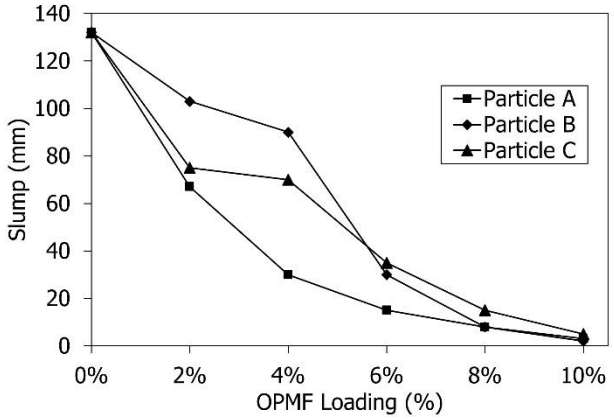

Fig 5: Effect of oil palm mesocarp fiber on the slump of produced fiber-concrete composite

B. Concrete Density

Concrete density is a crucial characteristic affecting cost, structural performance, durability, and thermal and acoustic qualities. Engineers and architects carefully evaluate the required density while developing structures to ensure that concrete meets each application's unique needs. Proper mix design, quality control, and construction techniques are imperative to attain the necessary density and guarantee the long-term performance of concrete structures. The density of both the non-fiber concrete and the concrete with fibers was determined according to the standard quoted above. This result is expressed in Fig 6, which shows the effect of fiber inclusion as river sand replacement by volume on the concrete densities produced with the different particle sizes A, B, and C, respectively. The obtained result shows a steady decrease in the density of concrete as the fiber content increases with the low density of fiber compared to that of river sand being responsible for this phenomenon. Fiber particle size A attained a reduction in concrete density which ranged between 1.23%, 0.51%, 1.07%, 3.71%, and

3.79% for 2%, 4%, 6%, 8%, and 10% fiber–sand replacement, respectively. Particle size B affects a reduction in density with 1.64%, 0.26%, 0.16%, 0.65%, and 0.83% representing percentage fiber-sand replacement of 2%, 4%, 6%, 8%, and 10% fiber load, respectively. The percentage reduction in density of OPMF-concrete fiber in comparison with that of non-fiber concrete using the particle size C was 1.43%, 1.13%, 1.02%, 0.596%, and 3.92% representing 2%, 4%, 6%,8%, and 10% respectively. Overall, particle fiber B performs variably well, as the percentage reduction is lower than the other particle sizes under consideration. The reduction in density pattern obtained in this work is consistent with other research work where sand content in concrete was partially replaced either with natural fiber or other waste materials ([8], [76]). A reduction in concrete density as shown in this study may result into reduction in structural strength, durability, and resistance to environmental factors.

C. Water Absorption

Fig 7 shows the graphical representation of the result obtained for the water absorption properties and porosity of the produced OPMF-concrete composite. Water absorption

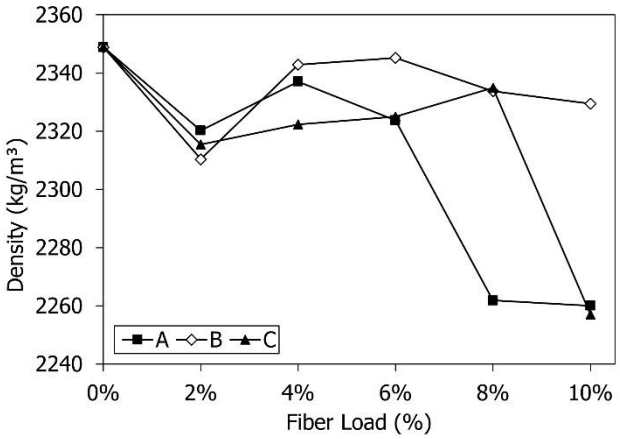

Fig 6: Density of OPMF-Concrete

is a crucial property of consideration for the durability of concrete as most chemical passage relies on the moisture within the concrete. From the result obtained, it can be seen that the water absorption of the produced fiber-concrete reduced compared to that of plain concrete, except for 8% fiber inclusion for fiber particle size A. Generally, the absorption value is reduced across all the percentage sand replacements. On-particle size basis, size A attained a water absorption reduction percentage value of 2.82%, 14.21%, 2.82%, and 4.23% for 2%, 4%, 6%, and 10% fiber loading, respectively, except for an increase in water absorption percentage at 8% which recorded an increase of 1.79%. Fiber particle size B recorded a varying decrease in the water absorption value across its percentage sand replacement, invariably increasing the reduction percentage compared to plain concrete, spread between 18.44% and 26.89%. A varying reduction percentage value of 7.68% to 21.38% was obtained for particle size C compared to ordinary concrete. It can be deduced from the obtained result that the reduction in water absorption by percent is due to the clogging of the available pore spaces within the concrete by the fiber, thereby reducing the passage of water within its structures.

It should be noted that particle size B has a consistent reduction percentage value and at a rate mostly higher than the remaining two particle sizes under consideration. Likewise, there is an increase in reduction percentage as the fiber content increases since more surface area of the fiber is present in the interspace of the composite concrete, thereby creating an avenue for the fiber to absorb the available water and also restricting cement hydration. This result contradicts that expressed by the research of [77], in which water absorption increases as the percentage of natural fiber inclusion in the mix increases, with no reference to the control sample expressed in the result. Comparing the result of this study with that of a research study [78] shows a similarity in the obtained water absorption percentage in glass fiber reinforced composite concrete in which the absorption reduces as a percentage increase in fiber inclusion as well as that obtained by [79], which shows a reduction in the water absorption properties of a rice husk ash composite-concrete. Generally, the graph showed an initial reduction in value from the control sample with no fiber and a steady rise in the increased of the water absorption as the fiber loading increased to optimum value at 8%, followed by a slight reduction at 10%; this exhibited a trend has similarity with that obtained by other researchers [80-81].

D. Porosity

From Fig 7, the graphical result of the effect of oil palm mesocarp fiber incorporation in concrete-on-concrete porosity can be obtained. The illustration shows a slight decrease in the porosity of OPMF-concrete from no-fiber concrete to 2% fiber–concrete and a steady increase in the porosity as fiber load content increases. The porosity obtained ranges from 16.3% to 22.16% across all fiber/sand.

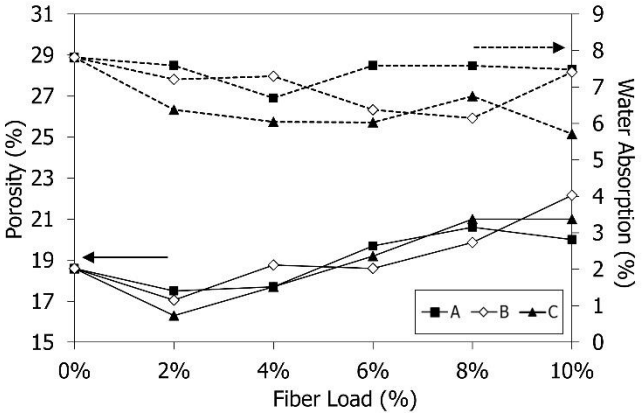

Fig 7: Porosity and water absorption of OPMF-Concrete

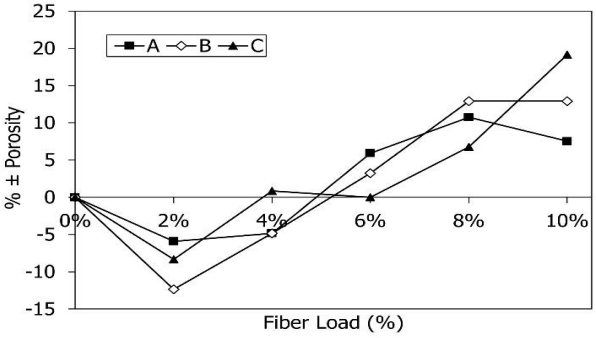

Fig 8: Percentage variation in porosity across fiber load

replacement percentages. The slight reduction in porosity occurred from 0% fiber–concrete at 18.6% to 16.3% at 2% fiber/sand replacement for particle size B, representing the most negligible percentage drop. The drop can be seen for 2% fiber content for other particle sizes too, and this is due to the clogging of pore spaces between the interphase of binder and aggregates (fine and coarse), thereby resulting in the reduction in pore spaces within the concrete microstructure which is responsible for porosity. The porosity of OPMF-concrete, in comparison to the control sample at 4% fiber content, also showed a decrease in value across the three distinct particle sizes. An increase in the porosity of OPMF-concrete is shown as the fiber content increase beyond 4% fiber load, that is, 6% fiber content and above. A steady rising trend path is established for the porosity as the fiber load increases. The increase in fiber content affords the fiber-concrete the possibility of more pores within the fiber particles to absorb more free water due to the hydrophilic tendency of the fiber. More fiber means more pore spaces within the fiber particle for water intake. Fig 8 shows the percentage difference the OPMF-concrete attained from the control specimens. This increase in porosity is similar to that obtained by [82], although non-natural fiber was used as the reinforcing component (i.e., steel fiber, polypropylene, and glass fiber), while the result from this study also corroborates that of [83], in which steady increase was obtained as natural fiber used content in their produced concrete increases.

E. Compressive Strength

Fig 9 illustrates the combined graphical representation of the average compressive strength of three specimens of the oil palm mesocarp fiber reinforced concrete with fiber particle sizes A, B and C as previously specified. The result shows the significant influence on the compressive strength of the concrete from the graph, and it can be seen that a reduction in strength occurs when the fiber is added to the plain concrete at certain days of curing. Particle size A result as illustrated in the A section of the result graph in fig 9, recorded a slight increase of compressive strength at curing age 7 days between no fiber and 2% fiber content from, with 39.167 MPa at no fiber to 40.33 MPa at 2% fiber/sand replacement. This slight increase amounts to a 2.97% increase in strength. This phenomenon could result from the slight reduction in pore spaces in the samples as the fiber lodges inside the available spaces and increases the fiber-cement matrix interphase, thereby enhancing the binding of the fiber to other components of the concrete. Despite this slight increase in the compressive strength of OPMF-concrete at age 7 days, the result shows a subsequent reduction in strength across other ages of testing. No fiber concrete possesses compressive strength of 48.63 MPa, 49.67 MPa and 61.67 MPa at 14, 28 and 56 days cured age while OPMF-concrete with 2% fiber content recorded compressive strength values of 41 MPa, 45 MPa and 56.73 MPa attained at 14, 28 and 56 days cured age respectively. Comparison between no fiber concrete and 2% OPMF-concrete shows a decline of 15.69%, 9.39%, and 8.00% at 14 days, 28 days, and 56 days, respectively.

Increasing the OPMF content to 4% shows a reduction in the compressive strength of the OPMF-concrete at the various testing ages compared to the control sample. The result from the 4% fiber inclusion shows the attainment of compressive strength in the range of 36.167 MPa to 52.333 MPa. In comparison to that obtained for the control specimen, the result shows a reduction in strengths across all testing ages valued at 7.66%, 28.03%, 22.16%, 15.14% for 7 days, 14 days, 28 days, and 56 days. The reduction in compressive strength of the OPMF-concrete in comparison to plain concrete can be associated with the increase in the fiber load, which increases the surface area of fiber-to-cement matrix interphase leading to the reduction in the binding of cement to both fine and coarse aggregate, thereby resulting in low strength. The subsequent increase in OPMF loading percentage shows a steady trend of reduction in compressive strength, as seen in the graph 6%, 8%, and 10% oil palm mesocarp fiber increases led to reductions in the compressive strengths of the concrete. The compressive strength at age 56 days produced a linear trend for the percentage of fine aggregate replacement by fiber. The values obtained are 61.67 MPa to 40.2 MPa at 0% and 10% fiber/sand replacement, respectively.

From the result obtained as illustrated in fig 9 above, it can be deduced that despite the apparent reduction in strength as the fiber load increases, the OPMF-concrete produced attained the designed compressive strength for all the percentage fine aggregate replacement at testing age of 28 days with values of 49.67 MPa, 45 MPa, 38.67 MPa, 35.83 MPa, 35.93 MPa and 31.3 MPa representing 0%, 2%, 4%, 6%, 8% and 10% fiber/sand replacement respectively.

Fig 9 section B of the graph illustrates the effect of OPMF particle size B replacement of fine aggregate on the compressive strength of the produced OPMF-concrete. The obtained compressive strength values expressed in the graph followed the same pattern as expressed in section A of Fig 9 with slight variation in value. At the testing age of 7 days, the obtained strengths are 39.16 MPa, 37 MPa, 35.3 MPa, 35 MPa, 33.93 MPa, and 30.27 MPa which represents compressive strength at 0%, 2%, 4%, 6%, 8%, and 10% fiber load respectively. 48.63 MPa, 41.167 MPa, 39.87 MPa, 37.7 MPa, 35.8 MPa and 33.93 MPa was recorded for 14 days cured specimens. At 28 days of standard testing age, compressive strengths are 49.67 MPa, 43.47 MPa, 42.47 MPa, 40.33 MPa, 42.17 MPa, and 36.13 MPa, representing values obtained at 0%, 2%, 4%, 6%, 8%, and 10% fiber load respectively. While at 56-day compressive strength stood at 61.67 MPa, 48.4 MPa, 45.93 MPa, 45. 37 MPa, 44.9 MPa and 38.33 MPa for 0%, 2%, 4%, 6%, 8%, and 10% fiber load respectively. OPMF particle size B asserts the same effect on the OPMF-concrete as the graphs show a steady decrease in compressive strength across all percentage fiber/sand replacement. The result obtained shows that adding fiber particle size B to concrete led to the reduction of compressive strengths compared to control specimens. Percentage reduction in compressive strength ranges from 5.53% to 21.5% for 2% fiber/sand replacement across 7, 14, 28, and 56 days of testing age. A steady reduction percentage of 22.72% to 37.84% at 7 days across to 56 days testing age was obtained for 10% OPMF loading.

As for particle size C, Fig 9 section C shows the effect of particle size C on the compressive strength of OPMF-concrete. Practically all obtained compressive strength result attained by the concrete with regards to the increase in fiber load exhibits a linear reduction trend in the strength. 36 MPa to 20.5 MPa was obtained for 7 days of testing across percentage fiber/sand replacement of 2% to 10%, 36.5 MPa to 20.67 MPa at 14 days testing age, 40.83 MPa to 23.17 MPa for 28 days testing age while 52.43 MPa to 24.5 MPa

was obtained at 56 days testing age, all with exclusion of the control specimen's compressive strength which reads 39.17 MPa, 48.63 MPa, 49.67 MPa and 61.67 MPa at 7, 14, 28 and 56 days respectively. The graph obtained is linear and only varied in value compared to other particle sizes (A and B) under consideration. The reduction in compressive strength can be attributed to the retardation of the hydration of cement binder in the concrete caused by the absorption of free water by the fiber, thereby restricting or reducing the formation of the C-S-H bonding within the microstructure of the concrete. Increasing fiber content leads to a gradual decrease in the hydration reaction, leading to a consistent decrease in the strength value. In a comparative analysis with no fiber concrete, OPMF-concrete with particle C, expresses a linear percentage reduction. At curing age 7 days, 8.1% to 47.66% reduction percentage was recorded compared to control specimen, across 2% to 10% fiber/sand replacement, with 10% fiber inclusion attaining the highest reduction percent. 24.94% to 57.5% at 14 days, 17.79% to 53.36% for 28 days of testing, while 56 days of testing age amounts to 14. 97% to 60.27% across all the replacement percentages of 2%, 4%, 6%, 8% and 10% respectively.

In general, the addition of fibers makes concrete more heterogeneous and less workable, resulting in inadequate compaction and increased voids. With an increase in OPMF content, concrete loses its workability.

The compacted concrete density may be slightly impacted by thin OPMF filaments' tangling and lower specific gravity/density in the cementitious matrix [84]. Additionally, because OPMF is hydrophilic as other natural plant-based fibers, it can absorb water from a fresh matrix, which reduces workability. This study's reduction in compressive strength is in line with that obtained by [85], in which jute fiber (natural fiber) was incorporated in slag concrete. Likewise, the addition of OPMF influences the hydration of cement; as the fiber inclusion increases, so does the retardation of hydration, resulting in a lower strength, as corroborated by [86]. However, the compressive strength of all the mixes increases with increasing curing ages. Using particle size B as a fair representative of all the produced OPMF-concrete, it can be seen, as expressed in Fig 10, that increase in the testing age leads to a corresponding increase in the compressive strength value obtained. The compressive strength obtained at 7 days rose by 36.48% at 56 days for the control sample, 23.55%, 23.1%, 22.85%, 24.43%, and 21.04%, representing a percentage increase from 7 days to 56 days for 2%, 4%, 6%, 8%, and 10% fiber load respectively. This trend is also obtained for the other two particle sizes (A and C). With increasing curing age for all mixes, compressive strength increased. The rates of strength increase were higher when the curing age increased from 7 to 28 days than when the curing age was increased from 28 to 56 days when comparing the strengths obtained at 7 and 56 days with those obtained at 28 days. The difference in percentage strength gained is because the first 28 days saw higher cement hydration rates than the later days; a similar trend is reported by other research [87-88].

Taking consideration of the designed compressive strength of M30 (30 MPa) at 28 days of testing, it can be deduced across all particle sizes that samples with sizes A and B attained the design strength at all percentage fiber inclusion of 2% to 10% while designed strength reduces for specimens with particle size C at fiber loading of 8% and 10%.

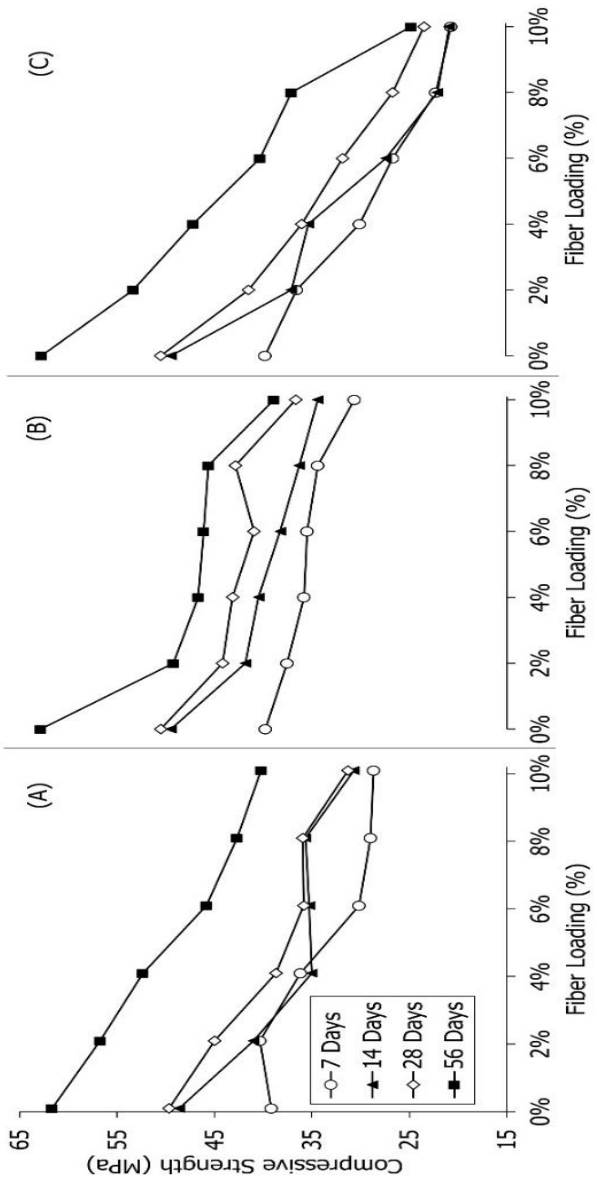

Fig 9: Compressive strength of OPMF-concrete with particle sizes (A) 0 – 1.18 mm, (B) 1.18mm - 2.35 mm, and (C) 2.35 mm - 5 mm

Table II expresses the analysis of variance conducted on the compressive strength values obtained at age 28 days. There is a significant difference in the values across ages of testing and all the percentage fiber/sand replacement, indicating the individual effects on the compressive strength at various fiber percent inclusion and fiber particle variations.

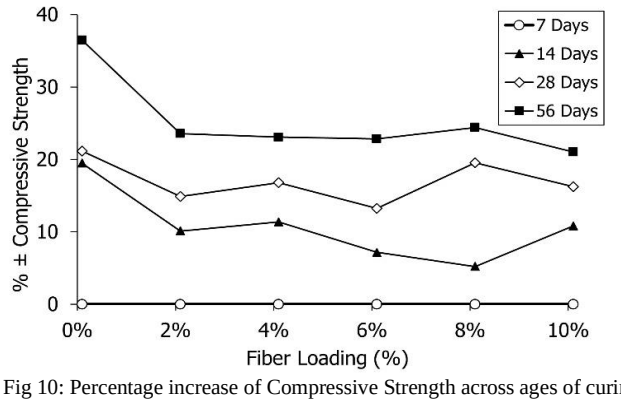

Fig 10: Percentage increase of Compressive Strength across ages of curing

TABLE II
ANALYSIS OF VARIANCE (ANOVA) ON COMPRESSIVE STRENGTH

SoV	SS	df	MS	F	P-value	F – crit
Rows	190.8	2	95.4	9.96	0.00417	4.10
Columns	705.5	5	141.1	14.7	0.000244	3.33
Error	95.8	10	9.6			
Total	992.1	17				

F. Flexural Strength

For the safety, effectiveness, and quality of structural elements in construction, it is essential to determine the flexural strength of concrete. It plays a crucial role in the planning, constructing, and upkeep of infrastructure and buildings, ultimately enhancing their durability and dependability. Fig 11 presents the effect of OPMF addition and content on the flexural strength and splitting tensile strength measured at 28 days. From fig 11 OPMF-concrete with fiber particle A exhibits a non-linear reduction flexural strength trend compared to the control specimens. An increase and decrease in the path can be seen from the graph as the fiber percentage increases. Across each percentage sand replacement, the flexural strength reduces with increasing fiber addition. The OPMF-concrete recorded flexural strength range value of 5.55 MPa to 4.71 MPa over all OPMF loading and percentage fine aggregate replacement. For particle size A, the flexural strength reduced by 15.18%, 7.49%, 14.64%, 3.12%, and 5.10% representing fiber percentages of 2, 4, 6, 8, and 10, respectively. Fiber size B exhibited a steady reduction in flexural strength at 2%, 4%, and 6% but with an increase in strength at 8% compared to the previous fiber load of the same particle size and a further drop in flexural strength at 10% fiber content. OPMF particle size B reduced flexural strength percentages by 2.40%, 8.34%, 12.36%, 3.42%, and 10.74%, representing 2%, 4%, and 6%. 8% and 10% fiber content, respectively. The flexural strength of fiber particle size C shows a similar pattern to that of particle size A, with a decrease in strength from 0% to 2% fiber content and an increase from 2% to 4% fiber content, after which a steady decrease in strength is attained as the fiber content increases. 11. 94%, 4.74%, 8.88%, 16.62%, and 13.69% represent the percentages reduction in strength in comparison to control at 2%, 4%, 6%, 8%, and 10% fiber load, respectively. Statistically, as shown in Table III, there is no significant difference in the flexural strength values attained by the various fiber contents and the fiber size.

G. Splitting Tensile

Concrete splitting tensile strength determination is essential for evaluating structural integrity, preventing cracking, maintaining quality, and optimizing construction practices. It is essential to the planning, constructing, and upkeep of infrastructure and buildings, ultimately enhancing their performance, durability, and safety. The maximum load recorded for each splitting tensile test was utilized to calculate the strength attained. Fig 11 shows the effect of oil palm mesocarp fiber inclusion on the splitting tensile strength of the fiber-composite concrete. A variation in graph paths can be seen as the strength is non-linear. OPMF-concrete attained splitting tensile strength range of 3.45 MPa to 2.23 MPa at the various particle sizes and fiber/sand replacement percentages compared to 3.13 MPa with no fiber. Fiber particle size A influences the splitting tensile strength by increasing the strength with 2% fiber inclusion and a steady slight reduction across other percentage fiber inclusion compared to that obtained at 2%. Fiber size B reduces strength at 2% from 0% fiber, a further reduction at 4%, and a steady rise to 8% fiber load with a later reduction at 10% fiber content. As for fiber particle size C, a drastic reduction in splitting tensile strength occurred at 2% fiber content but with a gradual increase in strength from the 2% content to 8% fiber inclusion and a further decrease at 10% fiber content. In terms of percentage reductions across all fiber sizes and loading, particle size A attained an increase in splitting tensile strength percentage of 10.22%, 5.05%, 6.10% at 2%, 4%, and 6%, respectively, to 0% at 8%, with a reduction in strength of 11.53% at 10% fiber content. Particle size B attained a reduction percentage of 1.71%, 9.91%, 6.11% at 2%, 4%, and 6% fiber content, respectively, a short increase of 2.02% at 8% and a further reduction of 11.19% at 10% fiber load. Particle fiber C reduced splitting tensile strength by 22.05%, 15.60%, 11.54%, 12.21%, and 28.82%, representing 2%, 4%, 6%, 8%, and 10% fiber content. Due to the formation of voids in the matrix and improper compaction brought on by higher fiber contents, which decreased workability, the splitting tensile strength of OPMF-Concrete decreased at higher fiber contents. Also, observation from the result shows that the splitting tensile strength decreases as the compressive strength of the OPMF-concrete reduces as the fiber loading increases. The pattern obtained in this study is similar to that

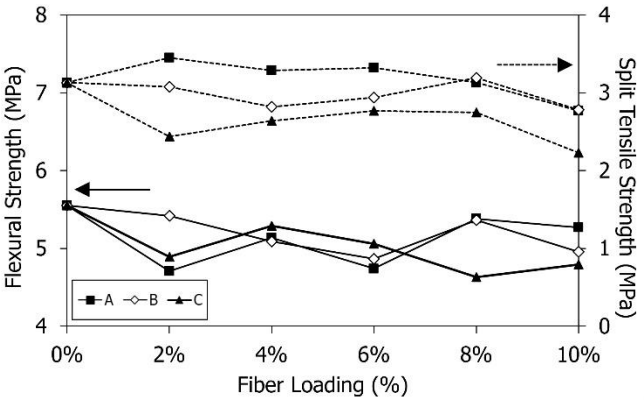

Fig 11: Flexural strength and splitting tensile strength of the three sizes of OPMF-concrete at 28 days of curing

TABLE III
ANALYSIS OF VARIANCE (ANOVA) ON FLEXURAL STRENGTH

SoV	SS	df	MS	F	P-value	F – crit
Rows	0.09	2	0.045	0.60282	0.566	4.103
Columns	0.81	5	0.16	2.179264	0.137881	3.326
Error	0.74	10	0.074			
Total	1.64	17				

TABLE IV
ANALYSIS OF VARIANCE (ANOVA) ON SPLITTING TENSILE STRENGTH

SoV	SS	df	MS	F	P-value	F – crit
Rows	0.836	2	0.417	10.93	0.00304	4.102821
Columns	0.515	5	0.103	2.69	0.085	3.325835
Error	0.382	10	0.0382			
Total	1.733	17				

reported by other research carried out on fiber/fiber derived ash incorporated concrete ([74], [89], [90]). Statistically as expressed in Table IV, there exist a significant difference in

the effect of percentages loading of fiber in the OPMF-concrete with p-value p<5% (0.00304) while there is no significant difference effect of OPMF particle sizes on the splitting tensile strength (p> 5%)

H. Morphological Test [SEM and EDX]

The SEM image analyses of the microstructures of the OPMF-modified concrete revealed that the addition of fiber had a significant effect on the concrete microstructures. Fig 12 (a-d), respectively, show the morphology of OPMF reinforced concrete containing 0% and 8% (particle sizes 0%, A, B, and C) as a fair representation for other percentage fiber inclusion as produced by the SEM micrographs. As shown in Fig. 12, the OPMF concrete has more pores than the control specimen. In addition, several needle-shaped crystals can be seen on the surface and surrounding the control sample. The inclusion of OPMF reduces the compressive strength value of concrete mixtures due to the OPMF specimens' lighter structure and larger pores within the fiber structure.

The EDX analyses of the specimens prepared with 8% OPMF as shown in Table V, revealed a steady decrease in the presence of silica proportion (SiO_2) as the fiber particle sizes increased, with the reduction percentages of 8.41%, 6.28%, and 7.53% representing the weight composition of silica proportion in 8A, 8B, and 8C OPMF-concrete, respectively, a drastic reduction when compared to the control specimen with 29.68% silica proportion. Reaffirming that inclusion of OPMF in the concrete reduces the SiO_2 content in the matrix. Also, the composition of Al_2O_3 decreased by 1.03, 1.24, and 2.70, representing 8A, 8B, and 8C, respectively. When compared to the control specimens, the carbon content as expressed by EDX shows a significant increase in proportion at 13.62%, 16.89%, and 23.95% representing OPMF-concrete with 8% fiber inclusion at particle size A, B, and C, respectively, as can be seen in table 6. It should be noted that the main difference between the 8% OPMF samples and the control was that the EDX spectrums had relatively small CaO, SiO_2, and Al_2O_3, implying that a tremendous amount of Ca and Al was replaced in the C-A-S-H chains.

The effect of fiber addition on the bond zone between paste and fiber is depicted in Fig. 12 (b-d). The bond zone between the OPMF particles grew in size and content as natural aggregates were replaced. The fiber content directly influences the number and size of cracks. The SEM results help to explain the sharp drop in the compressive strength with increasing OPMF content (from 0 to 8%) in the concretes matrix. The mechanical strength decrease can be attributed to bond defects between the fiber and the matrix, which are caused by the poor quality of the interfacial transition zone connecting the fiber particles and the cement paste [91]. Researchers [92] explained the reduced strength of fiber concrete in terms of a poor interface or transition zone, which resulted in micro-cracks at poor interface areas, which then expanded to a macro size, failing when compressed. apid Chloride Penetration Test.

The penetration of chlorides and other aggressive agents into the concrete affects the durability of concrete. The resistance of concrete to chloride ion penetration can be measured using the Rapid Chloride Permeability Test (RCPT). Variation in the chloride penetration resistance in terms of total charge passed is shown in Fig 13.

In this study, incorporating OPMF in concrete as a partial

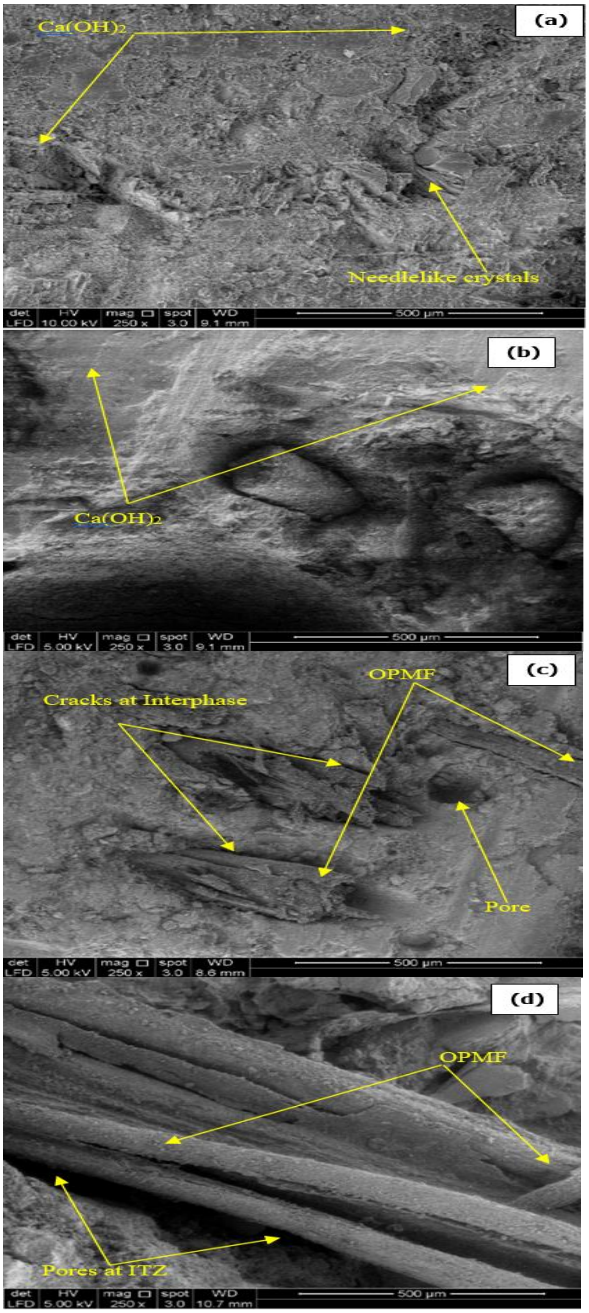

Fig 12. SEM images (a) 0% fiber-concrete, (b) 8% fiber-concrete of particle size A, (c) 8% fiber-concrete of particle size B, and (d) 8% fiber-concrete of particle size C

replacement for fine aggregate content significantly influences the chloride penetration of the produced concrete. At 2% fiber load for particle size A, a slight increase in the chloride permeability was attained in contrast to the control specimen, with a drop in penetration at 4% fiber load and a steady increase in penetration across the other percentage fiber loading arriving at 8.06%, -20.4%, -5.73%, 18.23% and 23.22% representing fiber loading of 2%, 4%, 6%, 8%, and 10% respectively. Fiber particle size B shows a consistent increase in the chloride penetration from 2% fiber load to 8% loading and then a slight decrease at 10%. Percentage comparison with the control samples shows a decrease percent of 24.13%, 3.35% 1.55% representing 2%, 4%, and 6% fiber load, respectively, and an increasing percentage of 21.93% at 8% fiber load, after which a slight reduction in percent was attained at 10% loading valued at 0.67%. Fiber particle size C shows a considerable increase

in the chloride penetration as values obtained are higher than the control.

Regarding percentage increase, 47.85%, 37%, 24.32%, 31.77%, and 29.75% representing 2%, 4%, 6%, 8%, and 10% fiber addition, respectively, were recorded. This study shows a variation in the chloride penetration achieved across fiber loading and fiber size. The result contradicts that reported when jute fiber is incorporated into concrete, as a reduction in the chloride penetration occurs [51]. No particular trend exists in the result obtained, but a significant influence was observed. A close similarity with the decrease in chloride penetration is presented in this study with OPMF particle size C when fly ash is used as a supplementary cementitious material, and the reduction is due to its pozzolanic attributes. Generally, from the graph obtained, aside from the initial drop in chloride penetration, a consistent increase was obtained as the fiber load increased, except for fiber particle size C which witnessed a high increase in chloride penetration and a subsequent reduction as the fiber loading increased. Overall, the result shows the charge passed (coulombs) of above 4000 coulombs for all specimens, control sample inclusive. Therefore, chloride ion penetrability is classified as high following the standard (ASTM C1202-12).

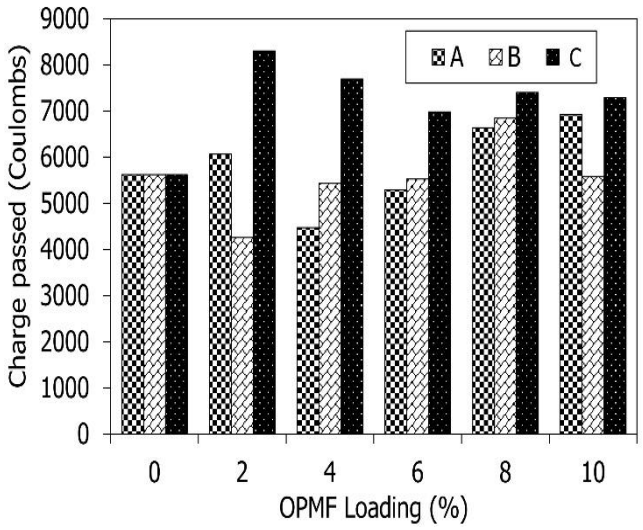

Fig 13. Rapid chloride penetration test

IV. CONCLUSION

The importance of environmental sustainability through the reuse or reduction of waste must be considered. This laboratory study was conducted to investigate the effectiveness of using OPMF as a constituent of concrete and to understand its effect on the workability, durability, morphological and mechanical properties of OPMF-incorporated concrete. The obtained results are summarized as follows:

1. All particle sizes utilized in this study reduce the slump by 22.12 % to 98.5%, depending on the particle size and the fiber loading in the concrete, with a fiber load of 10% attaining the most significant slump reduction. OPMFs absorb large amounts of water due to their high specific surface area, and the water needed for better flowability is reduced.

2. This study shows that adding OPMF to concrete reduces concrete density across all fiber loadings; the density obtained at the 28-day cured specimen ranged from 2320.2 to 2257 kg/m3, while the control specimen recorded a 2349 kg/m3. Despite the reduction, the OPMF-concretes have sufficient density. The negligible difference in concrete density is attested to by statistics showing no significant difference with p-value p - 0.174 across fiber loading and p - 0.06 across the three particle sizes, both greater than p< 5%

3. The addition of OPMF initially reduces the water absorption percentage of the OPMF-concrete, followed by a gradual increase as the fiber load increases. The concrete recorded a percentage increase of 1.79% and a reduction percent range of 2.81 to 26.89%, with the most negligible percentage reduction attained at 2% fiber load particle size A.

4. The effect of the addition of OPMF in concrete follows the same trend as that of water absorption, as there was a slight reduction in porosity at lower fiber loads and a steady increment in porosity subsequently. Porosity ranges from 17.5% to 22.16%, and the percentage change in porosity compared to control ranges from -5.91% to 19.14%.

5. The addition of OPMF recorded a compressive strength value range of 45 MPa to 23.17 MPa for all fiber loads and fiber sizes at 28 days. Comparing the compressive strength of the produced composite concrete to the control shows a reduction in value recorded at 49.67 MPa at 28 days, accounting for about 9.4% to 53.36% reduction in the compressive strengths at 28 days across particle sizes A, B, C, and percentage fiber loadings.

6. The flexural strength compared to control reduces from 2.40% to 15.18%, while splitting tensile strength takes an increase in values with a percentage range of 10.16 to 6.10

TABLE V
ELEMENTAL COMPOSITION OF 0% AND 8% OPMF-CONCRETE

Element	Weigth %	Atomic %	Compound %	Formula
CONTROL				
C K	0.00	0.00	0.00	CO_2
Na K	5.01	4.54	6.76	Na_2O
Al K	10.21	7.87	19.29	Al_2O_3
Si K	29.68	21.99	63.49	SiO_2
K K	2.36	1.25	2.84	K_2O
Ca K	5.45	2.83	7.62	CaO
O	47.29	61.52		
Total	100			
8A				
C K	13.62	20.63	49.91	CO_2
Mg K	0.76	0.57	1.27	MgO
Al K	1.03	0.69	1.94	Al_2O_3
Si K	8.41	5.45	17.99	SiO_2
S K	0.55	0.31	1.37	SO_3
Ca K	18.60	8.44	26.02	CaO
Fe K	1.16	0.38	1.50	FeO
O	55.87	63.52		
Total	100.00			
8B				
C K	16.89	25.56		
O K	51.68	58.70		
Al K	1.24	0.83		
Si K	6.28	4.06		
Ca K	23.92	10.84		
Total	100			
8C				
C K	23.95	33.59		
O K	51.05	53.75		
Mg K	0.94	0.65		
Al K	2.70	1.69		
Si K	7.53	4.52		
Ca K	13.82	5.81		
Total	100			

and a reduction range of 1.71 to 28.82% at various fiber loads and sizes, respectively.

7. SEM and EDX show the effect of OPMF on the interphases of the fiber with the cement matrix and aggregates. Cracks are evidence at the interphase of the creation of voids and a reduction in Ca and Al content in the C-A-S-H chains.

8. RCPT of all specimens produced achieves a charge above 4000 coulombs, classified as high chloride penetrability in the concrete without OPMF and that containing OPMF.

REFERENCES

[1] Huseien, G. F., Shah, K. W., & Sam, A. R. M. (2019). Sustainability of nanomaterials based self-healing concrete: An all-inclusive insight. *Journal of Building Engineering*, *23*, 155-171.

[2] Gregori, A., Castoro, C., Marano, G. C., & Greco, R. (2019). Strength reduction factor of concrete with recycled rubber aggregates from tires. *Journal of Materials in Civil Engineering*, *31*(8), 04019146.

[3] Huseien, G. F., Mirza, J., Ismail, M., Ghoshal, S. K., & Ariffin, M. A. M. (2018). Effect of metakaolin replaced granulated blast furnace slag on fresh and early strength properties of geopolymer mortar. *Ain Shams Engineering Journal*, *9*(4), 1557-1566.

[4] Huseien, G. F., Mirza, J., Ismail, M., & Hussin, M. W. (2016). Influence of different curing temperatures and alkali activators on properties of GBFS geopolymer mortars containing fly ash and palm-oil fuel ash. *Construction and Building Materials*, *125*, 1229-1240.

[5] Kubba, Z., Huseien, G. F., Sam, A. R. M., Shah, K. W., Asaad, M. A., Ismail, M., ... & Mirza, J. (2018). Impact of curing temperatures and alkaline activators on compressive strength and porosity of ternary blended geopolymer mortars. *Case Studies in Construction Materials*, *9*, e00205.

[6] Gupta, P. K., Khaudhair, Z. A., & Ahuja, A. K. (2016). A new method for proportioning recycled concrete. *Structural Concrete*, *17*(4), 677-687.

[7] Huseien, G. F., Hamzah, H. K., Sam, A. R. M., Khalid, N. H. A., Shah, K. W., Deogrescu, D. P., & Mirza, J. (2020). Alkali-activated mortars blended with glass bottle waste nano powder: Environmental benefit and sustainability. *Journal of cleaner production*, *243*, 118636.

[8] Mhaya, A. M., Huseien, G. F., Abidin, A. R. Z., & Ismail, M. (2020). Long-term mechanical and durable properties of waste tires rubber crumbs replaced GBFS modified concretes. *Construction and Building Materials*, *256*, 119505.

[9] Berardi, U., & Iannace, G. (2017). Predicting the sound absorption of natural materials: Best-fit inverse laws for the acoustic impedance and the propagation constant. *Applied Acoustics*, *115*, 131-138.

[10] Benmansour, N., Agoudjil, B., Gherabli, A., Kareche, A., & Boudenne, A. (2014). Thermal and mechanical performance of natural mortar reinforced with date palm fibers for use as insulating materials in building. *Energy and Buildings*, *81*, 98-104.

[11] Onésippe, C., Passe-Coutrin, N., Toro, F., Delvasto, S., Bilba, K., & Arsène, M. A. (2010). Sugar cane bagasse fibres reinforced cement composites: thermal considerations. *Composites Part A: Applied Science and Manufacturing*, *41*(4), 549-556.

[12] Yang, T., Hu, L., Xiong, X., Petrů, M., Noman, M. T., Mishra, R., & Militký, J. (2020). Sound absorption properties of natural fibers: A review. *Sustainability*, *12*(20), 8477.

[13] Arenas, J. P., del Rey, R., Alba, J., & Oltra, R. (2020). Sound-absorption properties of materials made of esparto grass fibers. *Sustainability*, *12*(14), 5533

[14] del Rey, R., Alba, J., Rodríguez, J. C., & Bertó, L. (2019). Characterization of new sustainable acoustic solutions in a reduced sized transmission chamber. *Buildings*, *9*(3), 60.

[15] Bakatovich, A., Davydenko, N., & Gaspar, F. (2018). Thermal insulating plates produced on the basis of vegetable agricultural waste. *Energy and Buildings*, *180*, 72-82.

[16] Belakroum, R., Gherfi, A., Kadja, M., Maalouf, C., Lachi, M., El Wakil, N., & Mai, T. H. (2018). Design and properties of a new sustainable construction material based on date palm fibers and lime. *Construction and Building Materials*, *184*, 330-343.

[17] Arenas, J. P., & Asdrubali, F. (2018). Eco-materials with noise reduction properties. *Handbook of Ecomaterials; Martinez, LMT, Kharissova, OV, Kharisov, BI, Eds*, 3031-3056.

[18] Belhadj, B., Bederina, M., Makhloufi, Z., Dheilly, R. M., Montrelay, N., & Quéneudéc, M. (2016). Contribution to the development of a sand concrete lightened by the addition of barley straws. *Construction and Building Materials*, *113*, 513-522.

[19] Azevedo, A. R. G., Cecchin, D., Carmo, D. F., Silva, F. C., Campos, C. M. O., Shtrucka, T. G., ... & Monteiro, S. N. (2020). Analysis of the compactness and properties of the hardened state of mortars with recycling of construction and demolition waste (CDW). *Journal of Materials Research and Technology*, *9*(3), 5942-5952.

[20] Al-Sodani, K. A. A., Al-Zahrani, M. M., Maslehuddin, M., Al-Amoudi, O. S. B., & Al-Dulaijan, S. U. (2021). Chloride diffusion models for Type I and fly ash cement concrete exposed to field and laboratory conditions. *Marine Structures*, *76*, 102900.

[21] Marvila, M. T., Alexandre, J., de Azevedo, A. R., & Zanelato, E. B. (2019). Evaluation of the use of marble waste in hydrated lime cement mortar based. *Journal of Material Cycles and Waste Management*, *21*(5), 1250-1261.

[22] Khan, M. U., Nasir, M., Al-Amoudi, O. S. B., & Maslehuddin, M. (2021). Influence of in-situ casting temperature and curing regime on the properties of blended cement concretes under hot climatic conditions. *Construction and Building Materials*, *272*, 121865.

[23] de Azevedo, A. R. G., Alexandre, J., Marvila, M. T., de Castro Xavier, G., Monteiro, S. N., & Pedroti, L. G. (2020). Technological and environmental comparative of the processing of primary sludge waste from paper industry for mortar. *Journal of cleaner production*, *249*, 119336.

[24] de Azevedo, A. R., Alexandre, J., Xavier, G. D. C., & Pedroti, L. G. (2018). Recycling paper industry effluent sludge for use in mortars: A sustainability perspective. *Journal of Cleaner Production*, *192*, 335-346.

[25] Nasir, M., Johari, M. A. M., Maslehuddin, M., & Yusuf, M. O. (2020). Magnesium sulfate resistance of alkali/slag activated silico-manganese fume-based composites. *Construction and Building Materials*, *265*, 120851.

[26] de Azevedo, A. R., Marvila, M. T., Tayeh, B. A., Cecchin, D., Pereira, A. C., & Monteiro, S. N. (2021). Technological performance of açaí natural fibre reinforced cement-based mortars. *Journal of Building Engineering*, *33*, 101675

[27] Marvila, M. T., Azevedo, A. R., Cecchin, D., Costa, J. M., Xavier, G. C., do Carmo, D. D. F., & Monteiro, S. N. (2020). Durability of coating mortars containing açaí fibers. *Case Studies in Construction Materials*, *13*, e00406.

[28] de Azevedo, A. R. G., Alexandre, J., Zanelato, E. B., & Marvila, M. T. (2017). Influence of incorporation of glass waste on the rheological properties of adhesive mortar. *Construction and Building Materials*, *148*, 359-368

[29] AlKhatib, A., Maslehuddin, M., & Al-Dulaijan, S. U. (2020). Development of high performance concrete using industrial waste materials and nano-silica. *Journal of Materials Research and Technology*, *9*(3), 6696-6711.

[30] de Azevedo, A. R. G., Marvila, M. T., da Silva Barroso, L., Zanelato, E. B., Alexandre, J., de Castro Xavier, G., & Monteiro, S. N. (2019). Effect of granite residue incorporation on the behavior of mortars. *Materials*, *12*(9), 1449.

[31] Amaral, L. F., Delaqua, G. C. G., Nicolite, M., Marvila, M. T., de Azevedo, A. R., Alexandre, J., ... & Monteiro, S. N. (2020). Eco-friendly mortars with addition of ornamental stone waste-A mathematical model approach for granulometric optimization. *Journal of Cleaner Production*, *248*, 119283.

[32] Oliveira, P. S., Antunes, M. L. P., da Cruz, N. C., Rangel, E. C., de Azevedo, A. R. G., & Durrant, S. F. (2020). Use of waste collected from wind turbine blade production as an eco-friendly ingredient in mortars for civil construction. *Journal of Cleaner Production*, *274*, 122948.

[33] Marvila, M. T., Alexandre, J., Azevedo, A. R. G., Zanelato, E. B., Xavier, G. C., & Monteiro, S. N. (2019). Study on the replacement of the hydrated lime by kaolinitic clay in mortars. *Advances in Applied Ceramics*, *118*(7), 373-380.

[34] Buratti, C., Belloni, E., Merli, F., Zanella, V., Robazza, P., & Cornaro, C. (2018). An innovative multilayer wall composed of natural materials: Experimental characterization of the thermal properties and comparison with other solutions. *Energy Procedia*, *148*, 892-899.

[35] Siqueira, F. F. S., Cosse, R. L., Pinto, F. A. N. C., Mareze, P. H., Silva, C. F., & Nunes, L. C. C. (2021). Characterization of Buriti (Mauritia flexuosa) Foam for Thermal Insulation and Sound Absorption Applications in Buildings. Buildings 2021, 11, 292.

[36] Lafond, C., & Blanchet, P. (2020). Technical performance overview of bio-based insulation materials compared to expanded polystyrene. *Buildings*, *10*(5), 81.

[37] Colorado, H. A., & Loaiza, A. (2017). Portland cement paste blended with pulverized coconut fibers. *Advances in Materials Science for Environmental and Energy Technologies VI*, *262*, 79.

[38] Balasubramanian, J. C., & Selvan, S. S. (2015). Experimental investigation of natural fiber reinforced concrete in construction industry. *International Research Journal of Engineering and Technology*, *2*(1), 179-182.

[39] Ardanuy, M., Claramunt, J., & Toledo Filho, R. D. (2015). Cellulosic fiber reinforced cement-based composites: A review of recent research. *Construction and building materials*, *79*, 115-128.

[40] Elenga, R. G., Dirras, G. F., Maniongui, J. G., Djemia, P., & Biget, M. P. (2009). On the microstructure and physical properties of untreated raffia textilis fiber. *Composites Part A: Applied Science and Manufacturing*, *40*(4), 418-422.

[41] Ramakrishna, G., & Sundararajan, T. (2005). Impact strength of a few natural fibre reinforced cement mortar slabs: a comparative study. *Cement and concrete composites*, *27*(5), 547-553.

[42] Claramunt, J., Fernández-Carrasco, L. J., Ventura, H., & Ardanuy, M. (2016). Natural fiber nonwoven reinforced cement composites as sustainable materials for building envelopes. *Construction and Building Materials*, *115*, 230-239.

[43] Asim, M., Abdan, K., Jawaid, M., Nasir, M., Dashtizadeh, Z., Ishak, M. R., & Hoque, M. E. (2015). A review on pineapple leaves fibre and its composites. *International Journal of Polymer Science*, *2015*.

[44] Agopyan, V., Savastano Jr, H., John, V. M., & Cincotto, M. A. (2005). Developments on vegetable fibre–cement based materials in São Paulo, Brazil: an overview. *Cement and Concrete Composites*, *27*(5), 527-536.

[45] Zhao, G. (2018). Assessment of potential biomass energy production in China towards 2030 and 2050. *International Journal of Sustainable Energy*, *37*(1), 47-66.

[46] Gea, S., Hutapea, Y. A., Piliang, A. F. R., Pulungan, A. N., Rahayu, R., Layla, J., ... & Saputri, W. D. (2023). A comprehensive review of experimental parameters in bio-oil upgrading from pyrolysis of biomass to biofuel through catalytic hydrodeoxygenation. *BioEnergy Research*, *16*(1), 325-347.

[47] Momoh, E. O., & Osofero, A. I. (2020). Recent developments in the application of oil palm fibers in cement composites. *Frontiers of Structural and Civil Engineering*, *14*, 94-108.

[48] Page, J., Khadraoui, F., Boutouil, M., & Gomina, M. (2017). Multi-physical properties of a structural concrete incorporating short flax fibers. *Construction and Building Materials*, *140*, 344-353.

[49] Javadian, A., Wielopolski, M., Smith, I. F., & Hebel, D. E. (2016). Bond-behavior study of newly developed bamboo-composite reinforcement in concrete. *Construction and Building Materials*, *122*, 110-117.

[50] Abu, A. K., Yalley, P. P. K., & Adogla, F. (2016). The use of raffia palm (Raffia Hookeri) piassava fibres as reinforcement of concrete. *International Journal of Engineering Science*, *5*(6), 1-6.

[51] Nambiar, R. A., & Haridharan, M. K. (2021). Mechanical and durability study of high performance concrete with addition of natural fiber (jute). *Materials Today: Proceedings*, *46*, 4941-4947.

[52] Chen, Y., Yu, Q. L., & Brouwers, H. J. H. (2017). Acoustic performance and microstructural analysis of bio-based lightweight concrete containing miscanthus. *Construction and Building Materials*, *157*, 839-851.

[53] Khan, M., Shakeel, M., Khan, K., Akbar, S., & Khan, A. (2022). A Review on Fiber-Reinforced Foam Concrete. *Engineering Proceedings*, *22*(1), 13.

[54] Grubeša, I. N., Marković, B., Gojević, A., & Brdarić, J. (2018). Effect of hemp fibers on fire resistance of concrete. *Construction and Building Materials*, *184*, 473-484.

[55] Khan, M., & Ali, M. (2018). Effect of super plasticizer on the properties of medium strength concrete prepared with coconut fiber. *Construction and Building Materials*, *182*, 703-715.

[56] Afraz, A., & Ali, M. (2021). Effect of Banana Fiber on Flexural Properties of Fiber Reinforced Concrete for Sustainable Construction. *Engineering Proceedings*, *12*(1), 63.

[57] Norrrahim, M. N. F. (2018). Superheated steam pretreatment of oil palm biomass for improving nanofibrillation of cellulose and performance of polypropylene/cellulose nanofiber composites. *Cellulose Nanofiber Composites*

[58] Nordin, N. I. A. A., Ariffin, H., Hassan, M. A., Shirai, Y., Ando, Y., Ibrahim, N. A., & Yunus, W. M. Z. W. (2017). Superheated steam treatment of oil palm mesocarp fiber improved the properties of fiber-polypropylene biocomposite. *BioResources*, *12*(1), 68-81.

[59] Norrrahim, M. N. F., Ariffin, H., Hassan, M. A., Ibrahim, N. A., Yunus, W. M. Z. W., & Nishida, H. (2019). Utilisation of superheated steam in oil palm biomass pretreatment process for reduced chemical use and enhanced cellulose nanofibre production. *International Journal of Nanotechnology*, *16*(11-12), 668-679.

[60] Zahari, M. A. K. M., Ariffin, H., Mokhtar, M. N., Salihon, J., Shirai, Y., & Hassan, M. A. (2015). Case study for a palm biomass biorefinery utilizing renewable non-food sugars from oil palm frond for the production of poly (3-hydroxybutyrate) bioplastic. *Journal of Cleaner Production*, *87*, 284-290.

[61] Ahmad Kuthi, F. A., Haji Badri, K., & Mohmad Azman, A. (2015). X-ray diffraction patterns of oil palm empty fruit bunch fibers with varying crystallinity. In *Advanced Materials Research* (Vol. 1087, pp. 321-328). Trans Tech Publications Ltd.

[62] ASTM C136/C136M-14; Standard Test Method for Sieve Analysis of Fine and Coarse Aggregates. ASTM International: West Conshohocken, PA, USA, 2014.

[63] ACI (American Concrete Institute) Committee 318. 2019. Building Code Requirements for Structural Concrete (ACI 318-19) and Commentary (ACI 318R-19). Farmington Hills, MI: ACI

[64] ASTM C 192/C 192M. Standard practice for making and curing concrete test specimens in the laboratory. American Society for Testing Materials; 2007.

[65] EN, B. S. (2019). 12390-2: 2009. *Testing hardened concrete. Making and curing specimens for strength tests*.

[66] ASTM. (2020). ASTM C143/C143M: Standard test method for slump of hydraulic-cement concrete. West Conshohocken, PA, USA: American Society of Testing and Materials

[67] ASTM International. (2013). ASTM C642-13. *Standard Test Method for Density, Absorption, and Voids in Hardened Concrete*.

[68] BSI. (2009). BS EN 12390-3: Testing hardened concrete. Part 3: Compressive strength of test specimens.

[69] ASTM, C. (2002). 78-02. Standard test method for flexural strength of concrete (using simple beam with third–point loading). *Annual Book of ASTM Standards, American Society for Testing and Materials*.

[70] ASTM C 496/C 496M-04, *Standard Test Method for Splitting Tensile Strength of Cylindrical Concrete Specimens*, American Standard Test Method, West Conshohocken, Penn, USA, 2004

[71] ASTM C1202. (2012). Standard test method for electrical indication of concrete's ability to resist chloride ion penetration. In *American Society for Testing and Materials* (Vol. 100, pp. 1-8).

[72] Yoon, J., Kim, H., Koh, T.and Pyo, S. (2020), Microstructural characteristics of sound absorbable porous cement-based materials by incorporating natural fibers and aluminum powder, Construction and Building Materials, 243, 118167, https://doi.org/10.1016/j.conbuildmat.2020.118167.

[73] Chen, Y., Wu, F., Yu, Q.and Brouwers, H. (2020), Bio-based ultra-lightweight concrete applying miscanthus fibers: Acoustic absorption and thermal insulation, Cement and Concrete Composites, 114, 103829, https://doi.org/10.1016/j.cemconcomp.2020.103829.

[74] Ahmad, W., Farooq, S. H., Usman, M., Khan, M., Ahmad, A., Aslam, F., ... & Sufian, M. (2020). Effect of coconut fiber length and content on properties of high strength concrete. *Materials*, *13*(5), 1075.

[75] Lee, S.W, C.L. Oh, M.R.M. Zain, N.A. Yahya, The use of oil palm fiber as additive material in Concrete, IOP Conf. Series: Materials Science and Engineering 431 (2018) 1–6, https://doi.org/10.1088/1757899X/431/4/042012

[76] Oancea, I., Bujoreanu, C., Budescu, M., Benchea, M., & Grădinaru, C. M. (2018). Considerations on sound absorption coefficient of sustainable concrete with different waste replacements. *Journal of Cleaner Production*, *203*, 301-312

[77] Abdullah, A. C., & Lee, C. C. (2017). Effect of treatments on properties of cement-fiber bricks utilizing rice husk, corncob and coconut Coir. *Procedia Engineering*, *180*, 1266-1273.

[78] Beigi, M. H., Berenjian, J., Omran, O. L., Nik, A. S., & Nikbin, I. M. (2013). An experimental survey on combined effects of fibers and nanosilica on the mechanical, rheological, and durability properties of self-compacting concrete. *Materials & Design*, *50*, 1019-1029.

[79] Hamzeh, Y., Ziabari, K. P., Torkaman, J., Ashori, A., & Jafari, M. (2013). Study on the effects of white rice husk ash and fibrous materials additions on some properties of fiber–cement composites. *Journal of environmental management*, *117*, 263-267.

[80] Ren, G., Yao, B., Ren, M., & Gao, X. (2022). Utilization of natural sisal fibers to manufacture eco-friendly ultra-high performance concrete with low autogenous shrinkage. *Journal of Cleaner Production*, *332*, 130105.

[81] Torkaman, J., Ashori, A., & Momtazi, A. S. (2014). Using wood fiber waste, rice husk ash, and limestone powder waste as cement replacement materials for lightweight concrete blocks. *Construction and building materials*, *50*, 432-436.

[82] Simões, T., Costa, H., Dias-da-Costa, D., & Júlio, E. N. B. S. (2017). Influence of fibres on the mechanical behaviour of fibre reinforced concrete matrixes. *Construction and Building Materials*, *137*, 548-556.

[83] Omoniyi, T. E., & Akinyemi, B. A. (2013). Permeability coefficient and porosity characteristics of bagasse fiber reinforced concrete. *Journal of Emerging Trends in Engineering and Applied Sciences*, *4*(1), 121-125.

[84] de Lima, T. E., de Azevedo, A. R., Marvila, M. T., Candido, V. S., Fediuk, R., & Monteiro, S. N. (2022). Potential of using Amazon natural fibers to reinforce cementitious composites: a review. *Polymers*, *14*(3), 647.

[85] Gulzar, M. A., Ali, B., Barakat, O., Azab, M., Najemalden, A. M., Salih Mohammed, A., & Alashker, Y. (2023). Influence of jute fiber on tensile, electrical, and permeability characteristics of slag concrete: a better, cheaper, and eco-friendly substitute for conventional concrete. *Journal of Natural Fibers*, *20*(1), 2170947.

[86] Chakraborty, S., Kundu, S. P., Roy, A., Adhikari, B., & Majumder, S. B. (2013). Effect of jute as fiber reinforcement controlling the hydration characteristics of cement matrix. *Industrial & Engineering Chemistry Research*, *52*(3), 1252-1260.

[87] Sharaky, I., Issa, U., Alwetaishi, M., Abdelhafiz, A., Shamseldin, A., Al-Surf, M., ... & Balabel, A. (2021). Strength and water absorption of sustainable concrete produced with recycled basaltic concrete aggregates and powder. *Sustainability*, *13*(11), 6277.

[88] Cuthbertson, D., Berardi, U., Briens, C., & Berruti, F. (2019). Biochar from residual biomass as a concrete filler for improved thermal and acoustic properties. *Biomass and bioenergy*, *120*, 77-83.

[89] Rahman, M. E., Muntohar, A. S., Pakrashi, V., Nagaratnam, B. H., & Sujan, D. (2014). Self compacting concrete from uncontrolled burning of rice husk and blended fine aggregate. *Materials & Design*, *55*, 410-415.

[90] Ali, M., Liu, A., Sou, H., & Chouw, N. (2012). Mechanical and dynamic properties of coconut fibre reinforced concrete. *Construction and Building Materials*, *30*, 814-825.

[91] Corinaldesi, V., Mazzoli, A., & Moriconi, G. (2011). Mechanical behaviour and thermal conductivity of mortars containing waste rubber particles. *Materials & Design*, *32*(3), 1646-1650.

[92] Ganesan, N., Raj, J. B., & Shashikala, A. P. (2013). Flexural fatigue behavior of self compacting rubberized concrete. *Construction and Building Materials*, *44*, 7-14.